Renewable and Sustainable Energy Reviews 14 (2010) 615–628

Contents lists available at ScienceDirect

Renewable and Sustainable Energy Reviews

journal homepage: www.elsevier.com/locate/rser

A review of materials, heat transfer and phase change problem formulation for latent heat thermal energy storage systems (LHTESS)

Francis Agyenim [a,*], Neil Hewitt [a], Philip Eames [b], Mervyn Smyth [a]

[a] *Centre for Sustainable Technologies, University of Ulster, Newtownabbey BT37 0QB, UK*
[b] *Electronic and Electrical Engineering, Loughborough University, Leicestershire LE11 3TU, UK*

A R T I C L E I N F O

Article history:
Received 4 August 2009
Accepted 19 October 2009

Keywords:
Phase change material (PCM)
Latent heat thermal energy storage (LHTES)
PCM container
Conduction/convection heat transfer

A B S T R A C T

This paper reviews the development of latent heat thermal energy storage systems studied detailing various phase change materials (PCMs) investigated over the last three decades, the heat transfer and enhancement techniques employed in PCMs to effectively charge and discharge latent heat energy and the formulation of the phase change problem. It also examines the geometry and configurations of PCM containers and a series of numerical and experimental tests undertaken to assess the effects of parameters such as the inlet temperature and the mass flow rate of the heat transfer fluid (HTF). It is concluded that most of the phase change problems have been carried out at temperature ranges between 0 °C and 60 °C suitable for domestic heating applications. In terms of problem formulation, the common approach has been the use of enthalpy formulation. Heat transfer in the phase change problem was previously formulated using pure conduction approach but the problem has moved to a different level of complexity with added convection in the melt being accounted for. There is no standard method (such as British Standards or EU standards) developed to test for PCMs, making it difficult for comparison to be made to assess the suitability of PCMs to particular applications. A unified platform such as British Standards, EU standards needs to be developed to ensure same or similar procedure and analysis (performance curves) to allow comparison and knowledge gained from one test to be applied to another.

Contents

1. Introduction

The quest for new technologies to avert the growing concern about environmental problems, the imminent energy shortage and the high cost of energy and new power plants has been a scientific

* Corresponding author. Tel.: +44 2890 368 227; fax: +44 2890 368 239.
E-mail address: fb.agyenim@ulster.ac.uk (F. Agyenim).

1364-0321/$ – see front matter © 2009 Elsevier Ltd. All rights reserved.
doi:10.1016/j.rser.2009.10.015

Nomenclature

A	area (m^2); thermal diffusivity ratio, $A = \alpha_s/\alpha_f$
a	equation coefficient
Bi	Biot number, $Bi = hr_o/\lambda$
B	solid subcooling parameter, $B = \lambda_s \Delta T_s/\lambda_f \Delta T_{sf}$
b	width of a rectangular PCM container (m)
C	instantaneous height-averaged cooling rate
C_p	specific heat capacity (kJ/kg K)
d	diameter (m)
Fo	Fourier number
f	liquid fraction of PCM melt
g	acceleration due to gravity (m/s)
Gr	Grashof number
H	enthalpy (J)
h	heat transfer coefficient (W/(m^2 K))
He	instantaneous, height-averaged melting rate
HTF	heat transfer fluid
k	thermal conductivity (W/m)
l	length (m)
M	instantaneous, height-averaged melting rate
m	mass (kg)
$\dot{m}$	mass flow rate (kg/s)
Pr	Prandtl number
PCM	phase change material
Q	energy or heat flow (J)
q	heat flux (W/m^2)
R	thermal resistance (K/W)
Ra	Rayleigh number
Re	Reynold's number
r	radius (m)
Ste	Stefan number or liquid superheating, $Ste = C\Delta T_f/\lambda T$,
T	temperature (°C or K)
ΔT	temperature difference (°C or K)
t	time (s)
Δt	time step (s)
v	velocity components (m/s)
V	volume (m^3)
v	velocity (m/s)
X_f	local volume fraction of fibers
x, y, z	x, y, z-component in a Cartesian coordinate system
Δx	space increment (m)
w	dimensionless geometric parameter defined by $1 + w = lA/V$
Z	fin height (m)

Greek symbols

δ	fin thickness (m); dimensionless front radius (interface position)
α	thermal diffusivity of PCM (m^2/s)
β	coefficient of volumetric expansion (K^{-1})
ρ	density (kg/m^3)
λ	latent heat of fusion (kJ/kg)
θ	angle (°)
δ	dimensionless front radius, $\delta = r/r_o$
Φ	dimensionless temperature difference
υ	dynamic viscosity (m^2/s)
μ	viscosity (kg/(m s))
ε	emissivity, emmittance
τ	dimensionless time

Subscripts and superscripts

C	convective
Cd	conductive
c	cylindrical
cr	critical
e	enclosure
eff	effective
eq	equivalent
f	fluid
$fiber$	fiber
fin	fin
$fric$	friction
H	heat transfer fluid
i	inner (inlet)
l	liquid
lag	lag
m	melting
max	maximum
o	outer (outlet)
p	PCM
r	rectangular container
ref	reference
s	solid
t	tube

concern over the last three decades. Central to the problem is the need to store excess energy that would otherwise be wasted and also to bridge the gap between energy generation and consumption. Latent heat thermal energy storage is particularly attractive technique because it provides a high energy storage density. When compared to a conventional sensible heat energy storage systems, latent heat energy storage system requires a smaller weight and volume of material for a given amount of energy. In addition latent heat storage has the capacity to store heat of fusion at a constant or near constant temperature which correspond to the phase transition temperature of the phase change material (PCM). The study of phase change materials was pioneered by Telkes and Raymond [1] in the 1940s but did not receive much attention until the energy crisis of late 1970s and early 1980s where it was extensively researched for use in different applications especially for solar heating systems [2–33]. Less attention was however given to phase change storage research after the energy crisis until it emerged again recently. Since the late 70s a number of studies have been conducted to assess the overall thermal behaviours of latent heat thermal storage systems [34–59]. Studies of phase change systems have investigated design fundamentals, system and process optimization, transient behaviour, and field performance. The research and development has been broad based and productive, concentrating on both the resolution of specific phase change materials and problems and the study of the characteristics of new materials. The major disadvantage, as reported by many researchers has been the low thermal conductivities possessed by many PCMs, leading to low charging and discharging rates (especially for the organic based materials). The development of a latent heat thermal energy storage system therefore involves the understanding of heat transfers/exchanges in the PCMs when they undergo solid-to-liquid phase transition in the required operating temperature range, the design of the container for holding the PCM

and formulation of the phase change problem. This paper reviews the studies conducted on phase change materials for different applications and reported in the open literature.

2. Phase change materials (PCMs)

Energy storage may be in the form of sensible heat in a liquid or solid medium, as heat of fusion (latent heat), or as chemical energy or products in a reversible chemical reaction. The classification of energy storage and the materials used are detailed in [51]. Chemical energy storage has not as yet been used in practical applications and both technical and economical questions have yet to be answered for some of the possibilities proposed. To date most of the studies conducted on storage materials have concentrated on sensible and latent heat storage systems. Studies conducted to compare phase change and sensible heat storages have shown that a significant reduction in storage volume can be achieved using PCM compared to sensible heat storage. Results of studies from Morrison and Abdel-Khalik [48] and Ghoneim [60] show that to store the same amount of energy from a unit collector area, rock (sensible heat storage material) requires more than seven times the storage mass of Paraffin 116 Wax (P116-Wax), five times the storage mass of medicinal paraffin and more than eight times the storage mass of $Na_2SO_4 \cdot 10H_2O$.

2.1. PCMs investigated

Several authors have carried out investigation into a wide range of PCMs, subdividing them into organic, inorganic, eutectics PCMs [61]. The main criteria that govern the selection of phase change heat storage materials are [51]:

- Possess a melting point in the desired operating temperature range (temperature range of application).
- Possess high latent heat of fusion per unit mass, so that a smaller amount of material stores a given amount of energy.
- High specific heat to provide additional significant sensible heat storage effects.
- High thermal conductivity, so that the temperature gradients for charging and discharging the storage material are small.
- Small volume changes during phase transition, so that a simple container and heat exchanger geometry can be used.
- Exhibit little or no subcooling during freezing.
- Possess chemical stability, no chemical decomposition and corrosion resistance to construction materials.
- Contain non-poisonous, non-flammable and non-explosive elements/compounds.
- Available in large quantities at low cost.

Table 1 lists the current companies that commercially produce over 100 PCMs. In addition to these, several PCMs have been proposed or studied by different researchers. A detailed list of PCMs studied or proposed for study can be found in [51,62–65]. Table 2 gives the thermophysical data for a range of typical and important PCMs studied or proposed for study by previous authors.

Table 1
Commercial PCM manufacturers in the world.

Manufacturer	PCM temperature range	Number of PCMs listed
RUBITHERM (www.rubitherm.de)	−3 °C to 100 °C	29
Cristopia (www.cristopia.com)	−33 °C to 27 °C	12
TEAP (www.teappcm.com)	−50 °C to 78 °C	22
Doerken (www.doerken.de)	−22 °C to 28 °C	2
Mitsubishi Chemical (www.mfc.co.jp)	9.5 °C to 118 °C	6
Climator (www.climator.com)	−18 °C to 70 °C	9
EPS Ltd (epsltd.co.uk)	−114 °C to 164 °C	61
Merck		

2.2. Classification of PCMs to melting temperature range and application area

The selection of an appropriate PCM for any application requires the PCM to have melting temperature within the practical range of application. Several application areas have been proposed for PCMs studied. Table 2 lists some of the target application areas for the selection of PCMs for study, as provided by the references in the open literature. From Table 2, it can be seen that most of the research on phase change problems have been carried out within the temperature range 0–65 °C suitable for domestic heating/cooling (Table 3).

3. PCM containers

Once the PCM has been selected based primarily on the temperature range of application, the next most important factors to consider are:

(i) the geometry of the PCM container and
(ii) the thermal and geometric parameters of the container required for a given amount of PCM.

Each of these factors has a direct influence on the heat transfer characteristics in the PCM and ultimately affects the melt time and the performance of the PCM storage unit.

To ensure long-term thermal performance of any PCM system, the size and shape of the PCM container must correspond to the melting time of the PCM and the daily insolation at a given location, if the source of energy is a solar collector. PCMs are typically placed in long thin heat pipes [102], cylindrical containers [100,103] or rectangular containers [66,91]. A survey of previously published papers dealing with LHTES reveals that two geometries commonly employed as PCM containers are the rectangular and cylindrical containers. The most intensely analysed LHTES unit is the shell and tube system, accounting for more than 70%. This is probably due to the fact that most engineering systems employ cylindrical pipes and also heat loss from the shell and tube system is minimal. Fig. 1 gives the schematics of the cylindrical and rectangular containers. Table 4 lists some of the references to the studies undertaken employing the two most common container geometries.

3.1. Configurations of cylindrical PCM containers

Three modes of cylindrical PCM container configurations are distinguished. The first is where the PCM fills the shell and the heat transfer fluid flows through a single tube (Fig. 1a) [60,80,98–100] designated the pipe model. In the second model the PCM fills the tube and the HTF flows parallel to the tube (Fig. 1b) [56,107,80]. According to Esen et al. [80], who studied the two models theoretically by comparing the effects of various thermal and geometric parameters; cylinder radii, total PCM volume, mass flow rates and inlet temperatures of HTF on the storage time recommended the pipe model because it recorded a shorter melt time. This was because the thicker the PCM mass, the longer the melt time of the PCM. An added advantage for the pipe model not mentioned is the fact that the pipe model has a lower heat loss rate to the environment because most heat supplied from the center ends up heating the PCM. The third cylinder model is the shell and tube system [60,99] commonly used to improve heat transfer in PCMs. Agyenim et al. [99] conducted an experimental energy storage system to compare horizontal shell and tube heat exchanger (4 tubes) and a pipe model incorporating a medium

Table 2
Thermophysical properties of PCMs investigated for different applications.

Compound	Reference(s)	Melting temp, T_m (°C)	Heat of fusion, λ (kJ kg^{-1})	Specific heat capacity, C_p (kJ kg^{-1} K^{-1})	Thermal conductivity, k (W m^{-1} K^{-1})	Density, ρ (kg m^{-3})
Water-ice	[66–70]	0	335	4.2	2.4 (liquid) 0.6	1000
GR25	[74]	23.2–24.1	45.3	1.2 (solid) 1.2 (liquid)	–	–
RT25–RT30	[72,73]	26.6	232.0	1.80 (liquid) 1.41 (solid)	0.18 (liquid) 0.19 (solid)	749 (liquid) 785 (solid)
n-Octadecane	[55,56,74–79]	27.7	243.5	2.66 (liquid) 2.14	0.148 (liquid) 0.190 (solid)	785 (liquid) 865 (solid)
$CaCl_2 \cdot 6H_2O$	[66,80,81]	29.9	187	2.2 (liquid) 1.4 (solid)	0.53 (liquid) 1.09 (solid)	1530 (liquid) 1710 (solid)
Rubitherm RT	[37]					
$Na_2SO_4 \cdot 10H_2O$	[60,80,81]	32, 39	180	2.0 (liquid) 2.0 (solid)	0.15 (liquid) 0.3(solid)	1460 (solid)
Paraffin wax	[72,80,81]	32–32.1	251	1.92(solid) 3.26(liquid)	0.514 (solid) 0.224 (liquid)	830
Capric acid	[82,83]	32	152.7	–	0.153 (liquid)	878 (liquid) 1004 (solid)
Polyethelene glycol 900 (PEG900)	[84]	34	150.5	2.26 (liquid) 2.26 (solid)	0.188 (liquid) 0.188 (solid)	1100 (liquid) 1200 (solid)
Lauric–palmitic acid (69:31) eutectic	[85]	35.2	166.3	2.41 (liquid) 1.77 (solid)		
Lauric acid	[82,85–87]	41–43	211.6	2.27(liquid) 1.76(solid)	1.6	1.76(solid) 0.862 (liquid)
Stearic acid	[61,87–89]	41–43 (67–69)*	211.6	2.27 (liquid) 1.76 (solid)	1.60 (solid)	862 (liquid) 1007 (solid)
Medicinal paraffin	[60]	40–44	146	2.3 (liquid) 2.2 (solid)	2.1 (liquid) 0.5 (solid)	830 (solid)
Paraffin wax	[90]	40–53				
P116-Wax	[55,60,80,81]	46.7–50	209	2.89 (liquid) 2.89 (solid)	0.277 (liquid) 0.140 (solid)	786 (solid)
Merck P56-58	[53]	48.86–58.06	250	2.37 (liquid) 1.84 (solid)	–	–
Commercial paraffin wax	[94]	52.1	243.5	–	0.15	809.5 (solid) 771 (liquid)
Myristic acid	[35,58,95]	52.2	182.6	–	–	–
Paraffin RT60/RT58	[93,94]	55 to 60	214.4–232	0.9	0.2	775 (liquid) 850 (solid)
Palmitic acid	[83,85,87,89,92,95]	57.8–61.8	185.4		0.162 (liquid)	850 (liquid) 989 (solid)
$Mg(NO_3)_2 \cdot 6H_2O$	[71,88]	89	162.8	–	0.490 (liquid) 0.611 (solid)	1550 (liquid) 1636 (solid)
RT100	[96]	99	168	2.4 (liquid) 1.8 (solid)	0.2 (liquid) 0.2 (solid)	770 (liquid) 940 (solid)
$MgCl_2 \cdot 6H_2O$	[71,97]	116.7	168.6	2.61 (liquid) 2.25 (solid)	0.570 (liquid) 0.704 (solid)	1450 (liquid) 1570 (solid)
Erythritol	[50,98–100]	117.7	339.8	2.61(liquid) 2.25(solid)	0.326 (liquid) 0.733 (solid)	1300 (liquid) 1480 (solid)
$Na/K/NO_3$ (0.5/0.5)	[54,65]	220	100.7	1.35	0.56	1920
$ZnCl_2/KCl$ (0.319/0.681)	[54,65]	235	198	–	0.8	2480
$NaNO_3$	[54,65]	310	172	1.82	0.5	2260
KNO_3	[54,65]	330	266	1.22	0.5	2110
NaOH	[54,65]	318	165	2.08	0.92	2100
KOH	[54,65]	380	149.7	1.47	0.5	2044
$ZnCl_2$	[54,65]	280	75	0.74	0.5	2907
$LiF–CaF_2$ (80.5:19.5) mixture	[101]	767	816	1770 (liquid) 1.770 (liquid)	1.70 (liquid) 3.8 (solid)	2390 (liquid) 2390 (solid)

– Not available.

Table 3
Target application areas for some PCMs studied.

Temperature range (°C)	PCMs studied/melting temperature (°C)	Target application area (rationale behind selection of PCM)
0–65 °C	Paraffins (−3 to 64), water/ice/0, stearic acid/41–43, n-octadecane/27.7	Storage for domestic heating/cooling (see list in Table 1). Passive storage in bio-climatic building/architecture. Thermal storage of solar energy. Application in off-peak electricity for cooling and heating. Protection of electrical devices.
80–120 °C	Erythritol/117.7; RT100 (99); $MgCl_2 \cdot 6H_2O$ (116.7)	Storage for the hot-side of $LiBr/H_2O$ absorption cooling system with generator temperature requirements of less that 120 °C [100].
>150	$NaNO_3$/310, KNO_3/330 NaOH/318, KOH/380 $ZnCl_2$/280	Storage for solar power plants based on parabolic trough collectors and direct steam generation.

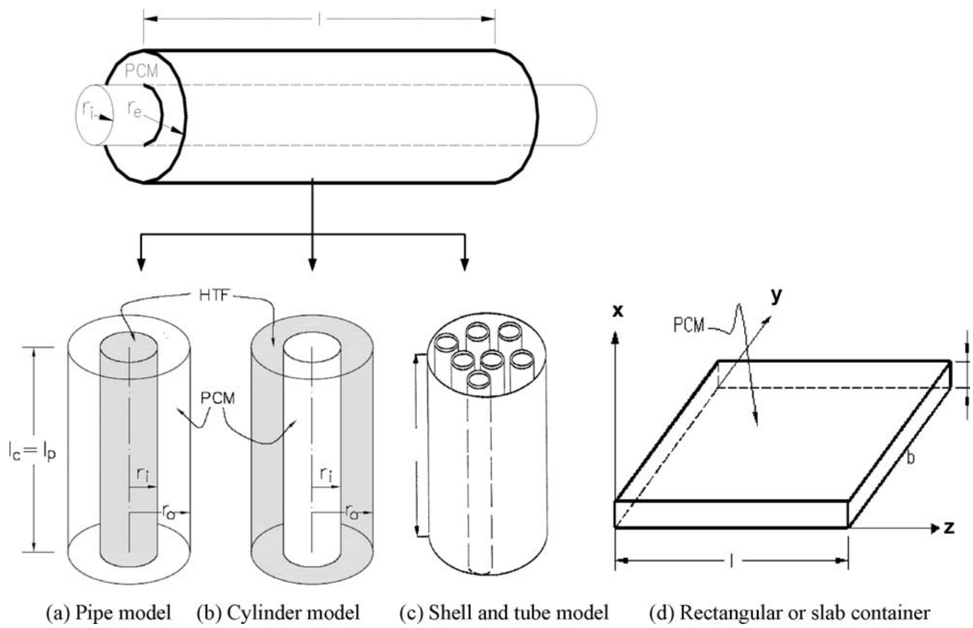


Fig. 1. Classification of commonly used PCM containers in terms of the geometry and configuration.

temperature phase change material (erythritol) with a melting point of 117.7 °C. The thermal characteristics in the systems were analysed using isothermal contour plots and temperature time curves. Temperature gradients along the three directions of the two systems; axial, radial and angular directions were also analysed and compared. Heat transfer in the shell and tube system was found to be dominated by the effect of multiple convective heat transfer compared to conductive heat transfer in the pipe model. The temperature gradients recorded in the axial direction for both the pipe and shell and tube systems during the change of phase were reported to be 2.5% and 3.5% that of the radial direction respectively, indicating essentially a two-dimensional heat transfer in both systems. The onset of natural convection through the formation of multiple convective cells in the shell and tube system significantly altered the shape of the solid liquid interface fluid flow and indicated complete melt time within 5 h compared to more than 8 h for the pipe model. The authors recommended the shell and tube system for the charging of PCMs.

Table 4
References to container geometry employed in the study of PCMs.

Geometry	Reference(s)
Cylindrical (concentric annulus)	[60,66,74,76,78,80,81,86,93,95, 97,102,106,107]
Cylindrical (shell and tube)	[56,75,90,101,104,105]
Rectangular/slab	[66,68,72,74,77,79,91,108]
Spherical	[74]

3.2. Counter-current and parallel HTF flow directions

In a cylindrical container assembly, two possibilities exist for the flow direction of the heat transfer fluid during charging and discharging of the PCM energy. The two modes are either the hot and cold fluids are introduced into the tube from the same end (parallel flow) or the hot and cold fluids are introduced from the opposite ends (counter-current flow) of the heat transfer tube during charging and discharging respectively. Fig. 2 illustrates the schematic diagram of the parallel and counter-current flow principles. For each pair, the upper arrow represents the direction of HTF flow during charging and the lower arrow represents discharge direction of the HTF.

Results from the numerical simulations conducted by Gong and Mujumdar [101] to investigate the effect of the parallel and counter-current flow modes using a mixture of 80.5% LiF and 19.5% CaF_2 as a PCM and He/Xe mixture as a HTF showed that parallel flow increases the energy charge/discharge rate by 5% more than counter-current flow. This was because the penetration depth of the solid–liquid phase change interface during the charge/discharge was larger due to higher temperature difference at the fluid inlet if hot and cold fluids enter from the same end. In addition, supercooling of the PCM did not occur in the fluid inlet region and heat transfer between the heat transfer fluid and the PCM did not deteriorate. On the other hand, counter-current flow for the charge/discharge processes produced significant supercooling of the PCM in the inlet region of the cold fluid.

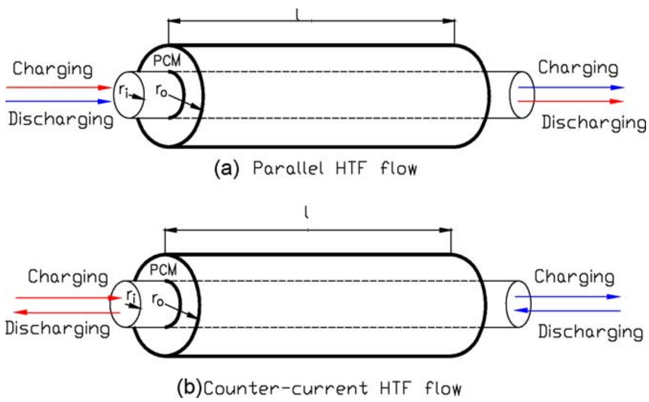


Fig. 2. The physical model illustrating parallel and counter-current HTF flow in a shell and tube system.

3.3. Investigating parameters in PCM containers

Apart from the container geometry and configuration, various thermal and geometric parameters are known to affect the thermal performance of LHTES. Table 5 lists the references to some of the operating parameters investigated and their key findings.

Key findings from numerical predictions, tested against experimental data for various operating parameters have shown that, in order to optimize the performance of a PCM storage unit, the thermal and geometric parameters listed in Table 5 must be carefully selected. Literature reviewed has shown a superior performance using the shell and tube configuration followed by the pipe model with the PCM at the shell side and the heat transfer fluid flowing through the center. It has therefore been recommended by many authors including [60,75,99,118].

4. Heat transfer in PCMs and enhancement techniques

Most PCMs have unacceptably low thermal conductivity, leading to slow charging and discharging rates, hence heat transfer enhancement techniques are required for most LHTES applications. Several studies have been conducted to study heat transfer enhancement techniques in phase change materials (PCMs) and include finned tubes of different configurations [59,69,94,97,98,102,109–112], bubble agitation [112], insertion of a metal matrix into the PCM [113,114], using PCM dispersed with high conductivity particles [115], micro-encapsulation of the PCM [116,117] or shell and tube (multitubes) [99,118]. Fig. 3 shows the pictures and drawings of some of the common heat transfer enhancement techniques studied. Table 6 lists some examples where enhancement techniques have been investigated.

Majority of the heat enhancement techniques have been based on the application of fins embedded in the phase change material. This is probably due to the simplicity, ease in fabrication and low cost of construction. This is followed by the impregnation of metal matrix into the PCM using high conductivity materials such as carbon fiber and brushes and multitubes. A selection of four studies where fins (circular and longitudinal), metal matrix and shell and tube systems approach have been adapted are described in Table 7. It can be seen from Table 7 that different approaches were used in the analysis with different results and interpretations.

The general observations drawn from the various studies demonstrate that, irrespective of the PCM used, the heat transfer characteristics of the PCMs can be improved using all of different enhancement techniques. Choi and Kim [97], Horbaniuc et al. [102], Velraj et al. [93] and Hamada et al. [75], employed different experimental setups, different container materials, and different PCMs to investigate the heat transfer enhancement characteristics of PCMs.

In terms of performances of heat transfer enhancement techniques and systems used by Choi and Kim [97], Horbaniuc et al. [102], Velraj et al. [93] and Hamada et al. [75], the best enhancement technique as reported in the literature was that due to Velraj et al. [93] where the effective thermal conductivity calculated employing paraffin with lessing rings was ten times ($2\ W\ m^{-1}\ K^{-1}$) greater than the thermal conductivity of paraffin ($0.2\ W\ m^{-1}\ K^{-1}$). This must be qualified by the fact that different researchers employed different experimental setups, different container materials, and different PCMs to investigate the heat transfer enhancement characteristics (Table 8). For example during the charging and discharging stages of the experiment, the heat transfer fluid in the experiment from Horbaniuc et al. [102] passed over just a fraction of the whole setup rendering heat addition and removal inefficient. Results derived from any such setup cannot be considered to be optimal.

Different researchers used different parameters to assess the heat transfer enhancement in the PCMs. Velraj et al. [93] evaluated the enhancement of the heat transfer using the effective thermal conductivity taken from a two-dimensional enthalpy-temperature governing equation which assumed no variation of temperature and thermal conductivity in the axial direction. Results were presented graphically using temperature–time curve and as such limits the application tending to other applications. Horbaniuc et al. [102] measured performances of fins in terms of the interface freezing stage and the time taken for complete solidification to be achieved using parabolic and exponential approximations. Hamada et al. [75] used the effective thermal conductivity proposed by Fukai et al. [126] to assess and compare results with the control system with no heat transfer enhancement. In the case of Choi and Kim [97], the key parameters used to assess the heat transfer enhancement of the circular finned system were the ratio of overall heat transfer coefficient in the finned and the unfinned tube systems. They reported a ratio of 3.5 for a surface area ratio of 3.2 between the finned and the unfinned tube systems. A comparison was also made by deriving a relationship for the ratio of the total amounts of heat recovered in the finned and unfinned tube systems correlated with dimensionless parameters of Fourier, Stefan and Reynolds with a correlation coefficient of 0.994 and a

Table 5
Examples of common operating parameters investigated in the study of phase change containers.

Reference(s)	Parameter(s) investigated	Findings
[56]	1. PCM cylinder (shell) radii 2. Mass flow rate 3. HTF inlet temperature	1. Increasing mass flow rate increases the heat transfer rate and the molten volume fraction. 2. Increasing inlet temperature rate increases the heat transfer rate and the molten volume fraction.
[66]	Comparison of rectangular and cylindrical containers	For larger quantities of PCM ($\geq$2 kg), the melting time of cylindrical container was nearly twice that of the rectangular one for equal volume and equal heat transfer.
[74]	Melt time	Average and total heat fluxes ($4852\ kJ/m^2$ and $-4403\ kJ/m^2$) approach the latent heat storage capacities per unit surface area as change in temperature approaches zero.
[101]	Effect of the parallel and counter-current flow modes	Energy charge/discharge rate for parallel flow is 5% more than counter-current flow mode

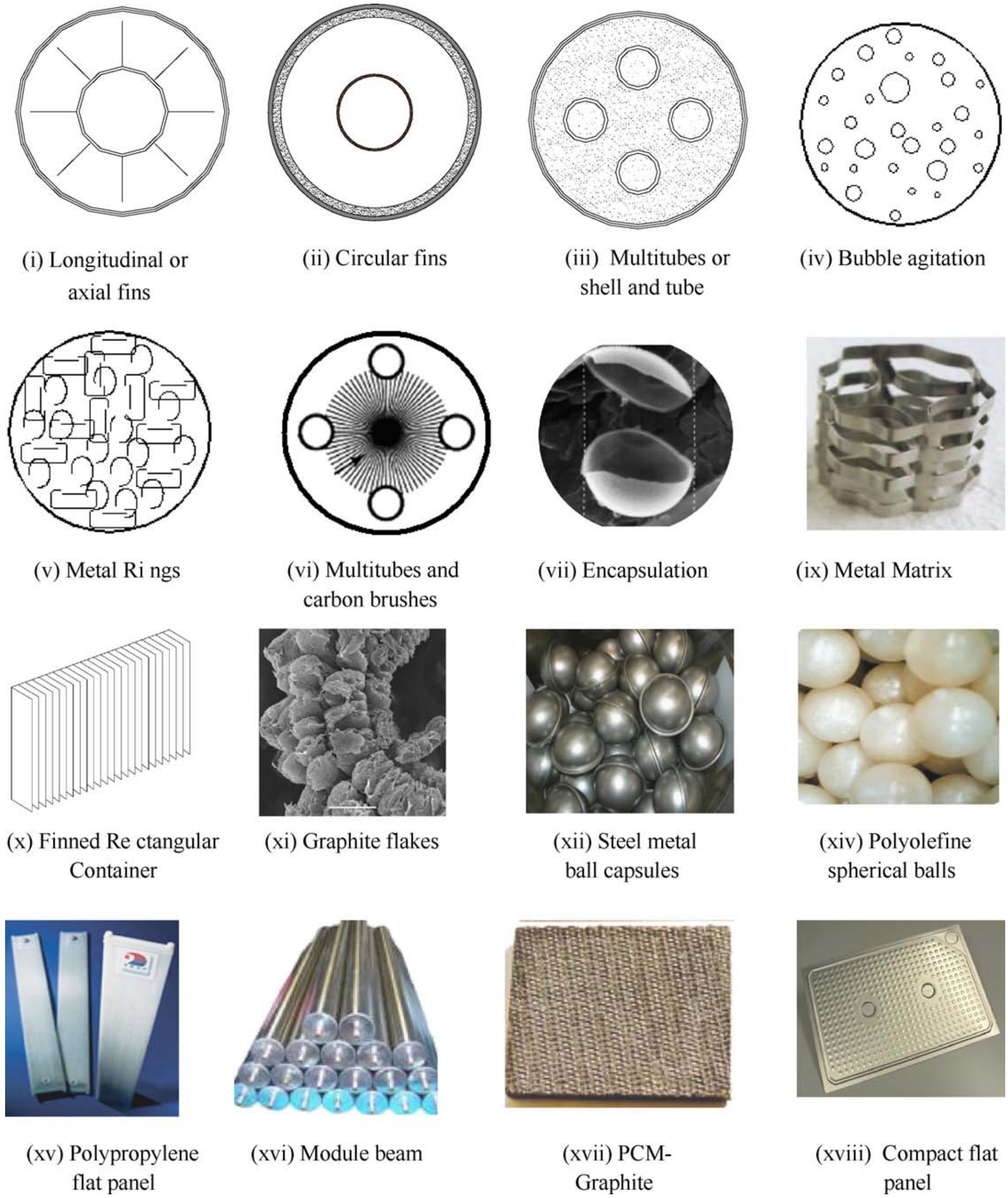


Fig. 3. Heat transfer enhancement methods employed in phase change material research.

Table 6
Heat transfer enhancement techniques employed in PCMs.

Reference(s)	Nature of study	Description of enhancement technique
[119]	Experimental	LiH PCM encapsulated in smaller container and placed in a bigger cylindrical container 5% Ni added uniformly to LiH.
[120]	Analytical	Aluminium and steel internal fins in the solidification of n-octadecane and salt-hydrate climsel.
[118]	Numerical and experimental	Staggered cylindrical tubes (multitubes) in a shell and tube system using Indonesian traditional substance called Mikro as a PCM.
[121]	Numerical	Plate type fins mounted on the vertical cooling surface of a rectangular vessel to study solidification of nitric molten salt.
[112]	Numerical and experimental	Internal longitudinal fins to improve heat transfer in paraffin PCM in a cylindrical container.
[122]	Experimental	A spiral twisted copper fins in a cylindrical tube to enhance heat transfer during the melting of stearic acid.
[110]	Numerical	Melting of ice in a porous medium surrounded by finned surfaces.
[79]	Numerical and experimental	System of 7 aluminium rectangular containers filled with n-octadecane and used as fins to improve heat transfer of PCM.
[123]	Analytical	Simplified analytical model to study heat transfer of fins and honeycombs in PCMs.
[124]	Experimental	Ultrasonic energy used to enhance heat transfer in Erythritol PCM.
[125]	Numerical	Micro-encapsulation of phase change slurries to improve convective heat transfer in the PCM.
[99,100]	Experimental	Internal longitudinal and circular fins and shell and tube system to improve heat transfer in Erythritol.

Table 7
A comparison of results of study using fins, metal matrix and shell and tube system.

Reference(s)	Heat enhancement technique	Method	Analysis and results	Observation or recommendation
[97]	Circular fins	Freezing of 0.36 kg weight $MgCl_2{\cdot}6H_2O$	Unfinned tube system:, $\frac{Q}{Q_{max}} = 2.39\times 10^{-2} Fo^{0.765} Ste^{0.528} Re^{0.195}, \; Re \le 7000$ Finned tube system: $\frac{Q}{Q_{max}} = 2.23\times 10^{-3} Fo^{0.781} Ste^{0.616} Re^{0.503}, \; Re \ge 7000$	Radial temperature gradient in the finned tube system is uniformly larger than the unfinned tube system. The axial temperature difference for the finned tube was smaller than for the unfinned tube in the liquid phase.
[102]	Longitudinal fins	Solidification of PCM (T_m = 60 °C)	Parabolic approximation of temperature profile: $t[a(t)]^2 = \frac{\lambda \rho k_s}{2k_{fin}^2 Z^2 \delta_{fin}} \left[\frac{Z}{2}\sqrt{\Delta T_{fin}} + \frac{\Delta T_{fin} - \Delta T_{fin}^2 a(t)}{2\sqrt{a(t)}} \ln \frac{2\sqrt{\Delta T_{fin} - Z^2 a(t)}}{\sqrt{\Delta T_{fin}} - 2Z\sqrt{a(t)}}\right]^2$ Exponential approximation of temperature profile: $-\Phi^{1/4} \ln \Phi = a_k x t^{-1/4}$, $\Phi = \frac{\Delta T(x,t)}{\Delta T_{fin}}$ and $a_k = \frac{2\lambda \rho_s k_s}{k_{fin}^2 \delta_{fin} \Delta T_{fin}}$	Ten fins would be sufficient to allow a complete solidification of PCM with T_m = 60 °C in an imposed freezing time of 180 min.
[93]	Fins, rings and bubble agitation	Solidification of Paraffin RT 60 and RT 58	Recommended internal longitudinal fins and lessing rings for solidification enhancement and the use of an evacuated tube for melting when using paraffin.	Effective thermal conductivity k_{eff} calculated by employing paraffin with lessing rings was $2\,W\,m^{-1}\,°C^{-1}$ (ten times greater than the thermal conductivity of paraffin).
[75]	Carbon fiber and brushes	Melting of PCM n-octadecane	Estimation of effective thermal conductivities using the semi-empirical equation from Fukai et al.: $\frac{k_{c.eff}}{k_p} = 0.456\{1-(1-X_{fiber})^{2/3}\}(k_{fiber}/k_p) + (1-X_{fiber})^{1/3}$	Heat brush/PCM composite was found to be inferior to the fiber-chip/PCM composite in terms of heat transfer rate of the bulk but the former was found superior to the latter in terms of overall heat transfer rate.

Table 8
Container materials used by previous researchers for PCM heat transfer enhancement.

Reference(s)	PCM container material and position	Heat transfer tube	Enhancement technique
[97]	Pyrex glass/vertical	Stainless steel tube	5 stainless steel circular fins
[102]	Horizontal	–	Longitudinal fins
[93]	Aluminium/vertical	Aluminium tube	Fins, rings, bubble agitation
[75]	Acrylic resin/vertical	4 steel tubes	Carbon fiber and brushes

standard deviation of 0.023 and 0.028, respectively. The above discussion illustrate the fact that there is no unified international or national standard methods (such as British Standards or EU standards) developed to test PCMs, making it difficult for comparison to be made to assess the suitability of PCMs to particular applications. A standard platform such as British Standards, EU standards needs to be developed to ensure same or similar procedure and analysis (performance curves) to allow comparison and knowledge gained from one test to be applied to another. Also contradictions exist in the thermophysical properties of PCMs provided especially the latent heat of fusion, thermal conductivity and densities in solid and liquid states. This is again due to the absence of unified certification standards and procedures.

5. Characterising the effect of melting and solidification rates in PCMs

To design PCM systems requires a good understanding of the fundamental heat transfer processes involved in accurately predicting the thermal performance of the PCM system. Based on both experimental and numerical investigations conducted to examine the thermal characteristics of LHTES systems, various correlations have been developed relating thermal performance and dimensionless numbers in given parametric domains. Dimensionless numbers are widely applied in modelling the PCM systems in order that the knowledge gained from one study can be extended beyond its source of acquisition. Among the thermal performance parameters for which correlations have been developed are melted volume fraction, temperature profile, melt time and melting rate. Table 9 gives the mathematical definitions of the common dimensionless numbers used in the study of LHTES systems and their significances to the phase change process. Table 10 gives references to some of the correlations derived using dimensionless numbers.

In spite of the significant literature available in quantifying melting and solidification rates, there has been no attempt to correlate available data. The two main reasons for this are:

- individual authors used different phase change materials with different heat transfer characteristics. In the case where the same PCM has been used, the researchers employed different dimensionless parameter ranges and presentations making it difficult to cross-correlate between the characteristics influencing the heat transfer in specific PCMs.
- some researchers presented results without using dimensionless parameters making it impossible to extend the knowledge to applications beyond the original source.

For example the empirical correlation for the melted volume fraction from Wang et al. [84], for example predicted the experimental data with an average error of 9.3% and the deviation was attributed to the sensible heating that takes place at the very early times due to the presence of subcooling within the PCM. In the case of the time averaged Nusselt number, the correlation was found to fit the individual experimental data with an average error of 8.8%. The dependency of the melted volume fraction on *Fo* and *Ste* but minimal for Ra was that, the dimensionless groups *Fo* and

Table 9
Definitions of some of the common dimensionless parameters employed in the analysis of phase change problems.

Number	Source	Formula	Significance (determination)
Biot, *Bi*	[126]	$Bi = \frac{hl}{k}$	Ratio of conductive to convective heat transfers resistance. Determines uniformity of temperature in solid.
Nusselt, *Nu*	[75,84]	$Nu = \frac{hd}{k}$	Ratio of the conductive thermal resistance to convective thermal resistance. Determines the ratio of actual heat transferred by a moving fluid to the heat transfer that would occur by conduction.
Stefan, *Ste*	[127]	$Ste = \frac{C_{p,l}\Delta T}{\lambda}$	Ratio of thermal capacity of the melted solid to the latent heat.
Dimensionless time or Fourier number, *Fo*	[75]	$\tau = \frac{kt}{\rho C_p l^2}$	Characterises heat flux into a body or system.
Rayleigh, Ra	[84]	$Ra = \frac{g\beta\Delta T l^3}{\alpha\upsilon}$	Determines the onset of convection. Below a critical value, heat transfer is primarily conduction.
Prandtl, Pr	[84]	$Pr = \frac{\nu}{\alpha}$	Approximates the ratio of momentum diffusivity to thermal diffusivity. Low Pr means effective heat conduction with dominant thermal diffusivity. High Pr means effective heat convection with dominant momentum diffusivity.
Reynolds number, Re	[122]	$Re = \frac{}{\upsilon}$	Ratio of inertial forces to viscous forces. Determines whether flow is laminar or trubulent.
Grashof number, *Gr*	[128]	$Gr = \frac{g\beta\Delta T l^3}{\upsilon^2}$	Approximates the ratio of buoyancy force to the viscous force.

Table 10
A list of some of the correlations derived by different references using dimensionless numbers.

Reference(s)	Correlation derived	Interpretation of correlation
[84]	$\frac{V}{V_o} = a(t - t_c)$	Linear function of the melted volume of PCM with time.
	$\frac{V}{V_o} = 4.73 Fo^{0.906} Ste^{1.538} \mathrm{Ra}^{0.002}$	Melted volume fraction for the entire duration of test runs in terms of *Fo*, *Ste* and Ra.
	$Nu = 0.219\,\mathrm{Ra}^{0.387}\,Pr^{0.019}\left(\frac{H}{\delta}\right)^{0.062}$	Time averaged Nusselt number for the entire melting process.
[74]	$t_f = \frac{l^2}{2\alpha(1+w)Ste}\{1 + (0.25 + 0.17w^{0.7})Ste\}$	Total heat input per unit surface area Q and average heat flux at $r = l$ over the duration of the melting process t_f.
	$\bar{q} = \frac{-2k\Delta T}{l}\{1 + (0.1210 + 0.0424w)Ste^{(0.7645-0.2022w)}\}$	
[78]	$k_{eq}(\tau) = 0.228\phi\,\mathrm{Ra}(\tau)^{1/4}\left[1 - \frac{d(\tau)}{d}\right]^{1/4}$	Equivalent thermal conductivity and dimensionless melting rate $[1 - A(\tau)]$.
	$A(\tau)[1 - \ln A(\tau)] = 1 - 4\int_0^{\tau} k_{eq}(\tau)d\tau$	
[108]	$M(\bar{t}) = \frac{1}{St}\int_0^1 \bar{\mu}_0(\bar{y},\bar{t})d\bar{y}$, $He(\bar{t}) = \int_0^1 \frac{2}{\delta}d\bar{y}$ $C(\bar{t}) = \int_0^1 \frac{2B}{\lambda}d\bar{y}$ with $M = He - C$	Instantaneous melting rate, instantaneous heating rate and instantaneous cooling.
[97]	$\frac{Q}{Q_{max}} = 2.39 \times 10^{-2} Fo^{0.765} Ste^{0.528}\,\mathrm{Re}^{0.195}$	Radial temperature gradient in the unfinned and finned tube PCM ($MgCl_2{\cdot}6H_2O$) system.
	$\frac{Q}{Q_{max}} = 2.23 \times 10^{-3} Fo^{0.781} Ste^{0.616}\mathrm{Re}^{0.503}$	

Ste were the important factors to consider in the phase change process.

The difficulty in comparing data was illustrated by Agyenim [96] by comparing the dependence of Nusselt number on Reynolds number for four independent investigators:

i. Hamada et al. [75] employed equation from Petukhov [129], Gnielinski [130].

$$Nu = \frac{(f_{fric}/2)(Re - 1000)Pr}{1 + 12.7\sqrt{f_{fric}/2}(Pr^{2/3} - 1)}$$

$$(3000 < Re < 10^6, 0.5 < Pr < 2000) \quad (1)$$

ii. Zhang and Faghri [111] employed empirical correlation proposed by Edwards and Jensen [131].

$$Nu = \frac{0.023(l/d_i)^{0.2}}{(1.35 - 0.35l/d_i)} Re^{0.8} Pr0.4 \quad (2)$$

with l/d_i calculated from available data as 0.50408.

iii. Sexana et al. [132] calculated the Nusselt number using equation 3.34 for turbulent flow.

$$Nu = 0.026 Re^{0.8} Pr^{1/3} \quad (3)$$

iv. Esen et al. [80] and Rohsenow et al. [133] employed Dittus–Boelter equation for turbulent flow:

$$Nu = 0.023\,Re^{0.8} Pr^{0.4} \text{ for } (Re > 2200) \quad (4)$$

Agyenim [96] illustrated that although all correlations showed the same general trend with an apparent slight differences in values recorded for the lower Reynolds numbers in the turbulent regime, major deviations increased with increased Nusselt and Reynolds numbers. Independent correlations presented demonstrated that in the turbulent region, the Nusselt number would be governed by the dimensionless parameters, $Nu = Nu(\mathrm{Re}, \mathrm{Pr})$ but data correlated only marginally well.

5.1. Phase change problem formulation

The analysis of heat transfer problems in phase change processes is complex due to the fact that the solid–liquid boundary moves depending on the speed at which the latent heat is absorbed or lost at the boundary. The position of the boundary is unknown and forms part of the solution Li et al. [134]. An increasing number of studies have been conducted and literatures on LHTES problems are numerous. Solutions to phase change problems include analytical, experimental and numerical using one-dimensional, two-dimensional or three-dimensional models to solve energy formulated equation. Energy equation is formulated in various ways with the phase change being accounted for in different representations. Examples of some of the formulation by various references are given in Table 11. Table 12 provides a list of references for the various solution methods employed in solving the phase change problems.

Table 11
Some examples of formulation for the phase change problem.

Reference(s)	Governing equation
[74]	$\frac{\partial T}{\partial t} = \frac{\alpha}{r^w}\frac{\partial}{\partial r}\left(r^w \frac{\partial T}{\partial r}\right)$ for $r(t) \le r \le l, T = T_{cr}, r \le r(t)$ where $1 + w = lA/V$ with $w = \begin{cases} 0 & \text{for a PCM slab insulated at one end} \\ 1 & \text{for a PCM cylinder} \\ 2 & \text{for a PCM sphere} \end{cases}$
[56]	$\frac{\partial H}{\partial t} = \frac{1}{r}\frac{\partial}{\partial r}\left(\alpha r \frac{\partial h}{\partial r}\right) + \frac{\partial}{\partial z}\left(\alpha \frac{\partial h}{\partial z}\right) - \rho \Delta h_f \frac{\partial f}{\partial t}$ $\rho C_p \pi r_i^2 \frac{\partial T}{\partial t} = 2\pi r_i U(T - T_H) - \dot{m} C_p \frac{\partial T}{\partial z}$ Phase change: $H(T) = h(T) + \rho_s f \Delta h_f$ where $h(T) = \int_{t_M}^{t} \rho C_p dT$
[101]	$\rho_H C_{p,H}\left(\frac{\partial T_H}{\partial t} + v \frac{\partial T_H}{\partial x}\right) = \frac{4h}{d}(T_P - T_H) + k_H \frac{\partial^2 T_H}{\partial x^2}$ $\frac{\partial H_P}{\partial t} = \left(\frac{1}{r}\right)\frac{\partial}{\partial r}\left(k_P r \frac{\partial T_P}{\partial r}\right) + \frac{\partial}{\partial x}\left(k_P \frac{\partial T_P}{\partial x}\right)$
[108]	Solid phase of PCM: $\frac{\partial T}{\partial t} + u_o \frac{\partial T}{\partial x} = \alpha_s \frac{\partial^2 T}{\partial x^2}$, liquid phase of PCM: $\frac{\partial u}{\partial x} + \frac{\partial v}{\partial y} = 0$ $v \frac{\partial^2 v}{\partial x^2} + g\beta(T - T_f) = 0$, $\frac{\partial T}{\partial t} + \frac{\partial}{\partial x}(uT) + \frac{\partial}{\partial y}() = \alpha_f \frac{\partial^2 T}{\partial x^2}$
[121,135]	Mass conservation equation: $\frac{\partial u_i}{\partial x_i} = 0$ Momentum conservation equations: $\rho\left(\frac{\partial u_i}{\partial t} + u_j \frac{\partial u_i}{\partial x_j}\right) = \frac{\partial \delta_{ij}}{\partial x_j} - \rho g \beta (T - T_{ref}) \frac{\partial x_2}{\partial x_i}$ where $\sigma_{ij} = -p\delta_{ij} + \mu\left(\frac{\partial u_i}{\delta x_j} + \frac{\partial u_j}{\partial x_i}\right)$ and $p' + \rho g x_2$ Conservation of energy: $\rho c\left(\frac{\partial T}{\partial t} + u_j \frac{\partial T}{\partial x_j}\right) = \frac{\partial}{\partial x_i}\left(k \frac{\partial T}{\partial x_j}\right)$
[112]	$\rho \frac{\partial H}{\partial t} = \frac{1}{r}\frac{\partial}{\partial r}\left(kr \frac{\partial T}{\partial r}\right) + \frac{1}{r}\frac{\partial}{\partial \theta}\left(\frac{k}{r}\frac{\partial T}{\partial \theta}\right)$ Phase change formula: solid region $(T \le T_m - \varepsilon)$: $H = c_p T$, interface $(T_m - \varepsilon \le T \le T_m + \varepsilon)$: $H = c_p T + \left(\frac{\lambda}{2\varepsilon}\right)T - T_m + \varepsilon$, liquid region $(T \ge T_m + \varepsilon)$: $H = c_p T + \lambda$

Table 12
Numerical, experimental and analytical solution and validation of phase change problems.

Reference(s)	Solution and validation	Nature
[66]	2D fixed-grid conjugate enthalpy based method. Finite difference and tridiagonal matrix algorithm solver.	Numerical and experimental.
[66]	1D enthalpy based method. Gauss–Seidel iteration procedure.	Numerical and experimental.
[80]	2D conjugate heat transfer enthalpy based method. Gauss–Seidel iteration procedure	Numerical.
[74]	1D enthalpy based method. Solved via Crank–Nicholson scheme.	Numerical.
[104]	1D enthalpy based method. Finite difference program-CYCLOP.	Analytical and Numerical.
[97]	–	Experimental.
[93]	1D and 2D enthalpy method. Implicit finite difference method.	Numerical and experimental.
[102]	1-Parabolic and exponential approximations for temperature profile. Newton–Raphson technique.	Analytical.
[75]	2D enthalpy method. Solved using the control volume method by Pantakar (1980).	Numerical and experimental.
[105]	2D fixed-grid conjugate enthalpy based method. Control finite difference method.	Numerical
[81]	2D enthalpy based method. Gauss–Seidel iteration procedure and TRNSYS.	Numerical
[72]	2D Navier–Stokes and energy equations. Finite element model.	Numerical and experimental.
[68]	1D and 2D fixed-grid enthalpy based method. Control volume approach by Pantankar (1980).	Numerical.
[86]	–	Experimental.
[91]	1D enthalpy based method.	Experimental.
[95]	–	Experimental.
[76]	Fixed-grid enthalpy–porosity model. Streamline upwind/Petrov Galerkin finite element method.	Numerical.
[106]	2D fixed-grid enthalpy method. Finite volume approach.	Numerical
[77]	2D enthalpy method. Solved using Ozisik.	Theoretical
[107]	1D enthalpy method.	Analytical.
[78]	–	Analytical and experimental.
[108]	2D mass, momentum and energy equations. Finite difference method.	Theoretical and experimental.
[79]	1D and 2D enthalpy method. Fully implicit finite difference method.	Numerical
[101]	2D energy based equation. Finite element analysis.	Numerical.
[60]	2D fixed-grid enthalpy based method. Gauss–Seidel iteration method.	Theoretical.
[90]	3D enthalpy based method. Control volume method by Patankar.	Experimental and numerical.

A survey of phase change formulation reveals that the most common approach applied in the solution of phase change problems is the formulation using the enthalpy method. The advantage of employing the enthalpy procedure has been reported as the removal of the need to satisfy conditions at the phase change front which most authors indicated facilitate the implementation of the numerical algorithm. The survey of publications from LHTES systems with cylindrical containers also shows that nearly half (47%) of the studies undertaken are numerical and half of the references employed two-dimensional models (Fig. 4).

Results from the numerical methods reported appear to show that they offer a good approach to solving the phase change problem although most of the available solutions to phase change problems apply to one- or two-dimensional systems due to the complexity of the equations involved in the phase change. The latent heat phase change problem has been assumed to be conduction controlled by some authors whereas natural convection in the liquid phase has been included in the analysis by other authors, adding to the complexity of the phase change problem. Few examples of phase change problem classification have been reported in Table 13.

The numerical formulation has also concentrated on resolving specific phase change material problems and to study the characteristics of proposed or new materials. They include:

- heat transfer during melting and solidification of PCM; evaluation of the temperature distribution inside PCM, interface transient location, and the effect of natural convection in the molten zone and,
- the overall thermal performance, system heat capacity, charging and discharging rates and storage temperatures.

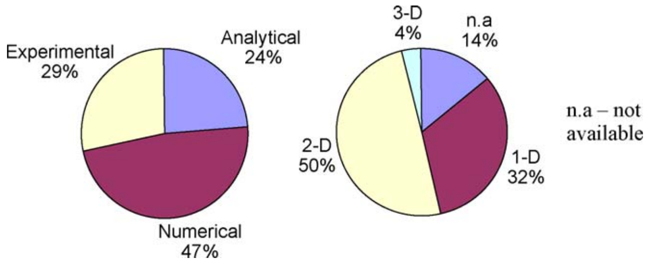


Fig. 4. Percentages of PCM solutions/analysis by methods and dimensions for 28 LHTES systems with cylindrical containers.

Table 13
PCM heat transfer control classification by different references.

Reference(s)	PCM	Control classification
[68]	Water-ice system	Conduction
[95]	95% purity palmitic acid	Conduction
[86]	95% purity lauric acid	Conduction
[76]	n-Octadecane	Convection
[106]	–	Convection
[77]	n-Octadecane	Conduction/convection
[107]	Paraffin wax, paraffin (p-116) and stearic acid	Conduction/convection
[78]	n-Octadecane	Conduction/convection

Table 14
Summary of method of analysis with key findings for conduction/convection control phase change problems.

Reference(s)	PCM/method	Parameters used to examine results	Key findings
[86]	Lauric acid. Pipe model with the PCM on the shell side and the heat transfer fluid flowing through the center of the tube.	Reynolds and Stefan numbers. Graphical presentation of temperature variations in radial and axial directions for different inlet HTF temperatures.	Charging time was less than solidification time due to: (i) melting rate being governed by convective heat transfer and (ii) conduction thermal resistance for the solidification process ($R_{cd} = r_H \ln(r/r_H)/2k_s$).
[78]	n-Octadecane. PCM inside an isothermally heated horizontal cylinder.	Ra and Pr numbers. Photographic samples at dimensionless times, τ. Graphical presentation of equivalent thermal conductivity equation derived to estimate dimensionless melting.	Melting proceeded faster than that of the pure heat conduction and heat transfer at the upper region of the PCM was larger than the lower region due to the presence of natural convection. However, decreasing Ra decreased convection and was negligible at $Ra < 10^5$.
[108]	n-Octadecane. PCM enclosed in a rectangular container and heated at a constant rate from one side.	*Nu*, thermal conductivity ratio A, solid subcooling B and *Ste*, Heating rate He and Melting rate, M. Graphical presentation of *Nu*, A, B, M and He.	*A* has practically no effect on the heating rate He during the convection dominated regime and has a minor impact on He during the conduction dominated regime. Higher *B* values produce lower melting velocities, especially in the early stage of the process. Melting rate decreases as *Ste* increases.

5.2. Classification of heat transfer characteristics

Problems that arise due to heat transfer accompanied by a change of phase can be classified as:

a. conduction controlled phase change,
b. convection controlled phase change or
c. conduction/convection controlled phase change.

References to some of the control classifications for some of the various studies reviewed are given in Table 13.

Studies based on the assumption that conduction is the major mechanism of heat transfer through the PCM assumed negligible convection heat transfer in the melt. In the case of convection controlled phase change, the common assumption was that the PCM was at the melting temperature. Models based on pure conduction and pure convection have not been able to predict accurately the melting rates nor track the complex motion of the solid–liquid interface at all times during the phase change. Less than 10% of articles surveyed treated convection and conduction at different stages and concluded that it depends on the phase transition stage to determine whether or not conduction or convection controls the heat transfer. Among these are Sari and Kaygusuz [86], Hirata and Nishida [78], Agyenim et al. [99] and Zhang and Bejan [108].

The authors accounted for both conduction and convection, making specifications at which times conduction/convection is (are) dominant during the phase change process. The details of the work by Zhang and Bejan [108] together with Sari and Kaygusuz [86], Agyenim et al. [99] and Hirata and Nishida [78] establish the following stages for the melting process:

a. Sensible heat provision at the start-up period during which heat added increases the temperature of the solid PCM. Pure conduction heat transfer occurs at this stage.
b. A second conduction regime, in which heat is purely transferred by conduction from the heated wall to the PCM and solid–liquid interface when melting had just begun.
c. The transition from conduction to natural convection which starts as the thickness of the melt layer increases and the interface starts to incline. At the interface, there exists at equilibrium, a solid body and a pool of its own liquid.
d. The convection regime, when most of the solid have been melted and the liquid core temperature distribution depends on height and depth and not on time (caused by buoyancy).

Phase change problems, first treated as pure conduction controlled, has in recent times moved to a different level of complexity with added convection in the melt being accounted for (Table 14).

6. Conclusion

Studies of phase change systems have over the past three decades investigated design fundamentals, system and process optimization, transient behaviour, and field performance. The research and development has been broad based and productive, concentrating on both the resolution of specific phase change materials and problems and the study of the characteristics of new materials. The review reveals the different heat transfer solution methods employed by different researchers. They include theoretical, experimental and numerical studies that have been conducted on the thermophysical properties of new phase change materials.

The following conclusions can be drawn from the models reported in the heat transfer and phase change problems reviewed:

- Most of the research on phase change problems has been carried out within the temperature range 0–60 °C suitable for domestic heating/cooling. Common PCMs studied are paraffins, Glauber's salts, wax, stearic acid and n-octadecane. Studies of medium temperature latent heat thermal energy systems to be applied for hot-side storage of absorption air conditioning are few.
- Most phase change materials have low thermal conductivities requiring heat transfer enhancement techniques to improve their rates of charging and discharging of energy. Majority of the studies undertaken on phase change materials have reported poor thermal conductivities requiring heat transfer enhancement techniques. As such current studies have concentrated on methods of heat transfer enhancement using mostly fins, insertion/dispersion of high thermal conductivity materials, multitubes and micro- or macro-encapsulation
- Numerical methods appear to offer a good approach to solving the phase change problem although most of the available solutions to phase change problems apply to one- or two-dimensional systems due to the complexity of the equations involved in the phase change.
- The latent heat phase change problem was first assumed to be conduction controlled. In recent times however, natural convection in the liquid phase has been included in the analysis of the phase change problem adding to the complexity of the phase change problem.
- A common approach observed in the solution of phase change problems has been the use of the enthalpy formulation. The advantage of the enthalpy procedure has been reported as the removal of the need to satisfy conditions at the phase change front to facilitate the implementation of the numerical algorithm.
- Variations are found to exist in correlations derived to characterise the effect of melting and solidification of PCMs. The variations have been attributed to the different methods of analysis and the choice of characteristic lengths used and as such calls for caution in the selection of correlation for design purposes and quantitative comparisons.
- There are no national and international standards for testing PCMs. As such researchers have over the years applied different approaches in both test procedures and analysis of results. The development of a unified international standard for test and analysis will be helpful in the development of latent heat thermal energy storage systems. Also contradictions exist in the thermophysical properties of PCMs provided especially the latent heat of fusion, thermal conductivity and densities in solid and liquid states. This is again due to the absence of unified certification standards and procedures.

References

[1] Telkes M, Raymond E. Storing solar heat in chemicals—a report on the Dover house. Heat Vent 1949;46(11):80–6.
[2] Telkes M. Thermal energy storage in salt hydrates. Solar Energy Materials 1980;2(4):381–93.
[3] Telkes M. Thermal storage for solar heating and cooling. In: Proceedings of the workshop on solar energy storage subsystems for the heating and cooling of buildings; 1975.
[4] Telkes M. Trombe wall with phase change storage material. In: Proceedings of the 2nd National Passive Solar Conference; 1978.
[5] Hodgins W, Qvale B, Swartman RK, Aureille R, Glew DN, Grjebine T, et al. Low temperature thermal energy storage. Energy 1977;2(1):70–5.
[6] Sparrow EM, Larson ED, Ramsey JW. Freezing on a finned tube for either conduction-controlled or natural-convection-controlled heat transfer. International Journal of Heat and Mass Transfer 1981;24(2):273–84.
[7] Kemink RG, Sparrow EM. Heat transfer coefficients for melting about a vertical cylinder with or without subcooling and for open or closed containment. International Journal of Heat and Mass Transfer 1981;24(10):1699–710.
[8] Pillai KK, Brinkworth BJ. The storage of low grade thermal energy using phase change materials. Applied Energy 1976;2(3):205–16.
[9] Jurinak JJ, Abdel-Khalik SI. On the performance of air-based solar heating systems utilizing phase-change energy storage. Energy 1979;4(4):503–22.
[10] Lorsch HG, Kauffman KW, Denton JC. Thermal energy storage for solar heating and off-peak air conditioning. Energy Conversion 1975;15(1–2):1–8.
[11] Jurinak JJ, Abdel-Khalik SI. Properties optimization for phase-change energy storage in air-based solar heating systems. Solar Energy 1978;21(5):377–83.
[12] Morrison DJ, Abdel-Khalik SI. Effects of phase-change energy storage on the performance of air-based and liquid-based solar heating systems. Solar Energy 1978;20(1):57–67.
[13] Hale Jr NW, Viskanta R. Solid–liquid phase-change heat transfer and interface motion in materials cooled or heated from above or below. International Journal of Heat and Mass Transfer 1980;23(3):283–92.
[14] Bareiss M, Beer H. An analytical solution of the heat transfer process during melting of an unfixed solid phase change material inside a horizontal tube. International Journal of Heat and Mass Transfer 1984;27(5):739–46.
[15] Feldman D, Shapiro MM, Fazio P, Sayegh S. The compressive strength of cement blocks permeated with an organic phase change material. Energy and Buildings 1984;6(1):85–92.
[16] Bhargava AK. A solar water heater based on phase-changing material. Applied Energy 1983;14(3):197–209.
[17] Ho CJ, Viskanta R. Inward solid–liquid phase-change heat transfer in a rectangular cavity with conducting vertical walls. International Journal of Heat and Mass Transfer 1984;27(7):1055–65.
[18] Jurinak JJ, Abdel-Khalik SI. Sizing phase-change energy storage units for air-based solar heating systems. Solar Energy 1979;22(4):355–9.
[19] Johnson TE. Lightweight thermal storage for solar heated buildings. Solar Energy 1977;19(6):669–75.
[20] Bell MA, Smith IE. Thermal energy storage using saturated salt solutions. Energy 1980;5(10):1085–90.
[21] Kimura H, Kai J. Phase change stability of $CaCl_2{\cdot}6H_2O$. Solar Energy 1984;33(1):49–55.
[22] Hill JE, Kelly GE, Peavy BA. A method of testing for rating thermal storage devices based on thermal performance. Solar Energy 1977;19(6):721–32.
[23] Marshall R, Dietsche C. Comparisons of paraffin wax storage subsystem models using liquid heat transfer media. Solar Energy 1982;29(6):503–11.
[24] Solomon AD. Design criteria in PCM wall thermal storage. Energy 1979;4(4):701–9.
[25] Solomon AD. On the melting of a simple body with a convection boundary condition. Letters in Heat and Mass Transfer 1980;7(3):183–8.
[26] Gueceri SI, Faunce SF. Modeling of a thermal wall panel using phase change materials. Energy 1979;4(4):695–9.
[27] Garg HP, Nasim M. Studies on low-temperature salt-hydrate for thermal storage applications. Energy Conversion and Management 1981;21(2):125–30.
[28] Kimura H, Kai J. Phase change stability of $CaCl_2{\cdot}6H_2O$. Solar Energy 1984;33(6):557–63.
[29] Marshall R. Parametric sensitivity studies using paraffin wax storage subsystems. Solar Energy 1984;32(1):41–8.
[30] Yoneda N, Takanashi S. Eutectic mixtures for solar heat storage. Solar Energy 1978;21(1):61–3.
[31] Katayama K, Saito A, Utaka Y, Saito A, Matsui H, Maekawa H, Saifullah AZA. Heat transfer characteristics of the latent heat thermal energy storage capsule. Solar Energy 1981;27(2):91–7.
[32] Knowles TR. Proportioning composites for efficient thermal storage walls. Solar Energy 1983;31(3):319–26.
[33] Miller WM. Energy storage via desiccants for food/agricultural applications. Energy in Agriculture 1983;2:341–54.
[34] Nagano K, Ogawa K, Mochida T, Hayashi K, Ogoshi H. Thermal characteristics of magnesium nitrate hexahydrate and magnesium chloride hexahydrate mixture as a phase change material for effective utilization of urban waste heat. Applied Thermal Engineering 2004;24:221–32.
[35] Sarı A. Eutectic mixtures of some fatty acids for low temperature solar heating applications: thermal properties and thermal reliability. Applied Thermal Engineering 2005;25:2100–7.
[36] Seeniraj RV, Narasimhan NL. Performance enhancement of a solar dynamic LHTS module having both fins and multiple PCMs. Solar Energy 2008;82:535–42.
[37] Stritih U. An experimental study of enhanced heat transfer in rectangular PCM thermal storage. International Journal of Heat and Mass Transfer 2004;47:2841–7.
[38] Akhilesh R, Narasimhan A, Balaji C. Method to improve geometry for heat transfer enhancement in PCM composite heat sinks. International Journal of Heat and Mass Transfer 2005;48:2759–70.
[39] Betzel T, Beer H. Experimental investigation of heat transfer during melting around a horizontal tube with and without axial fins. International Communications in Heat and Mass Transfer 1986;13(6):639–49.
[40] Butala V, Stritih U. Experimental investigation of PCM cold storage. Energy and Buildings 2009;41:354–9.
[41] Castell A, Sole C, Medrano M, Roca J, Luisa F, Cabeza LF, Garcıa D. Natural convection heat transfer coefficients in phase change material (PCM) modules with external vertical fins. Applied Thermal Engineering 2008;28:1676–86.

[42] Guo C, Zhang W. Numerical simulation and parametric study on new type of high temperature latent heat thermal energy storage system. Energy Conversion and Management 2008;49:919–27.
[43] Ismail KAR, Henriquez JR, Moura LFM, Ganzarolli MM. Ice formation around isothermal radial finned tubes. Energy Conversion & Management 2000;41: 585–605.
[44] Kayansayan N, Acar MA. Ice formation around a finned-tube heat exchanger for cold thermal energy storage. International Journal of Thermal Sciences 2006;45:405–18.
[45] Choi JC, Kim SD. Heat transfer in a latent heat-storage system using $MgC1_2{\cdot}6H_2O$ at the melting point. Energy 1995;20(1):13–25.
[46] Choi JC, Kim SD, Han GY. Heat transfer characteristics in low-temperature latent heat storage systems using salt-hydrates at heat recovery stage. Solar Energy Materials and Solar Cells 1996;40:71–87.
[47] Duffie J, Beckmann WA. Solar engineering of thermal processes. New York: John Wiley and Sons; 1991. p. 414–418, 506–507, 514, 669–683.
[48] Morisson, Abdel-Khalik. Effects of phase-change energy storage on the performance of air-based and liquid-based solar heating systems. Solar Energy 1978;20:57–67.
[49] Agyenim F, Eames P, Smyth M. A comparison of heat transfer enhancement in medium temperature thermal energy storage heat exchanger using fins and multitubes. ISES Solar World Congress 2007;2726–30.
[50] Agyenim F, Smyth M, Eames PC. A review of phase change material energy storage; selection of materials suitable for energy storage in the 100–130 °C temperature range. In: World Renewable Energy Congress (WREC 2005); 2005.p. 384–9.
[51] Abhat A. Low temperature latent heat thermal energy storage: heat storage materials. Solar Energy 1983;30(4):313–32.
[52] Voller VR. Fast implicit finite-difference method for the analysis of phase change problems. Numerical Heat Transfer Part B 1990;17:155–69.
[53] Akgun M, Aydın O, Kaygusuz K. Thermal energy storage performance of paraffin in a novel tube-in-shell system. Applied Thermal Engineering 2008;28:405–13.
[54] Pincemin S, Olives R, Py X, Christ M. Highly conductive composites made of phase change materials and graphite for thermal storage. Solar Energy Materials & Solar Cells 2008;92:603–13.
[55] Adine HA, El Qarnia H. Numerical analysis of the thermal behaviour of a shell-and-tube heat storage unit using phase change materials. Applied Mathematical Modelling 2009;33:2132–44.
[56] Lacroix M. Numerical simulation of a shell and tube latent heat thermal energy storage unit. Solar Energy 1993;50(4):357–67.
[57] Dincer I, Rosen MA. Thermal energy storage, systems and applications. Chichester (England): John Wiley & Sons; 2002.
[58] Sharma SD, Iwata T, Kitano H, Sagara K. Thermal performance of a solar cooker based on an evacuated tube solar collector with a PCM storage unit. Solar Energy 2005;78:416–26.
[59] Abdel-Wahed RM, Ramsey JW, Sparrow EM. Photographic study of melting about an embedded horizontal heating cylinder. International Journal of Heat and Mass Transfer 1979;22:171–3.
[60] Ghoneim AA. Comparison of theoretical models of phase-change and sensible heat storage for air and water-based solar heating systems. Solar Energy 1989;42(3):209–20.
[61] Sharma A, Tyagi VV, Chen CR, Buddhi D. Review on thermal energy storage with phase change materials and applications. Renewable and Sustainable Energy Reviews 2009;13:318–45.
[62] Lane G. Latent heat materials, vol. 1. Boca Raton, FL: CRC Press; 1983.
[63] Kenisarin M, Mahkamov K. Solar energy storage using phase change materials. Renewable and Sustainable Energy Reviews 2007;11:1913–65.
[64] Verma P, Varun, Singal SK. Review of mathematical modeling on latent heat thermal energy storage systems using phase-change material. Renewable and Sustainable Energy Reviews 2008;12:999–1031.
[65] Zalba B, Marín JM, Cabeza LF, Mehling H. Review on thermal energy storage with phase change: materials, heat transfer analysis and applications. Applied Thermal Engineering 2003;23(3):251–83.
[66] Zivkovic B, Fujii I. An analysis of isothermal phase change material within rectangular and cylindrical containers. Solar Energy 2001;70(1):51–6.
[67] Hawlader MNA, Wahed MA. Analyses of ice slurry formation using direct contact heat transfer. Applied Energy 2009;86:1170–8.
[68] Laouadi A, Lacroix M, Galanis N. A numerical method for the treatment of discontinuous thermal conductivity in phase change problems. Numerical Method for Heat and Fluid Flow 1998;8(3):265–87.
[69] Ermis K, Erek A, Dincer I. Heat transfer analysis of phase change process in a finned-tube thermal energy storage system using artificial neural network. International Journal of Heat and Mass Transfer 2007;50:3163–75.
[70] Inada T, Zhang X, Tabe A, Kozawa Y. Active control of phase change from supercooled water to ice by ultrasonic vibration 1. Control of freezing temperature. International Journal of Heat and Mass transfer 2001;44:4523–31.
[71] Nagano K, Takeda S, Mochida T, Shimakura K. Thermal characteristics of a direct heat exchange system between granules with phase change material and air. Applied Thermal Engineering 2004;24:2131–44.
[72] Huang MJ, Eames PC, Norton B. Thermal regulation building-integrated photovoltaics using phase change materials. Heat and Mass Transfer 2004;47(12-13):2715–33.
[73] Trp A, Lenic K, Frankovic B. Analysis of the influence of operating conditions and geometric parameters on heat transfer in water-paraffin shell-and-tube latent thermal energy storage unit. Applied Thermal Engineering 2006;26:1830–9.
[74] Solomon AD. Melt time and heat flux for a simple PCM body. Solar Energy 1979;22:251–7.
[75] Hamada Y, Ohtsu W, Fukai J. Thermal response in thermal energy storage material around heat transfer tubes: effect of additives on heat transfer rates. Solar Energy 2003;75:317–28.
[76] Ng KW, Gong ZX, Mujumdar AS. Heat transfer in free convection-dominated melting of a phase change material in a horizontal annulus. Heat Mass Transfer 1998;25(5):631–40.
[77] Hamdan MA, Elwerr FA. Thermal energy storage using phase change material. Solar Energy 1996;56(2):183–9.
[78] Hirata T, Nishida K. An analysis of heat transfer using equivalent thermal conductivity of liquid phase during melting inside an isothermally heated horizontal cylinder. Heat Mass Transfer 1989;32(9):1663–70.
[79] Costa M, Budhi D, Oliva A. Numerical simulation of a latent heat thermal energy storage system with enhanced heat conduction. Energy Conversion Management 1998;39(3/4):319–30.
[80] Esen M, Durmus A, Durmus A. Geometric design of solar-aided latent heat store depending on various parameters and phase change materials. Solar Energy 1998;62(1):19–28.
[81] Esen M, Ayhan T. Development of a model compatible with solar assisted cylindrical energy storage tank and variation of stored energy with time for different phase change materials. Energy Conversion and Management 1996;37(12):1775–85.
[82] Shilei L, Neng Z, Guohu F. Eutectic mixtures of capric acid and lauric acid applied in building wallboards for heat energy storage. Energy and Buildings 2006;38:708–11.
[83] Sharmaa A, Wona LD, Buddhi D, Park JU. Numerical heat transfer studies of the fatty acids for different heat exchanger materials on the performance of a latent heat storage system. Renewable Energy 2005;30:2179–87.
[84] Wang Y, Amiri A, Vafai K. An experimental investigation of the melting process in a rectangular enclosure. Heat and Mass Transfer 1999;42: 3659–72.
[85] Tuncbileka K, Saria A, Tarhanb S, Ergunes G, Kaygusuz K. Lauric and palmitic acids eutectic mixture as latent heat storage material for low temperature heating applications. Energy 2005;30:677–92.
[86] Sari A, Kaygusuz K. Thermal and heat transfer characteristics in a latent heat storage system using lauric acid. Energy Conversion and Management 2002;43:2493–507.
[87] Sarı A. Thermal reliability test of some fatty acids as PCMs used for solar thermal latent heat storage applications. Energy Conversion and Management 2003;44:2277–87.
[88] Domanski R, El-sebaii A, Jaworski M. Cooking during off-sunshine hours using PCMs as storage media. Energy 1995;20(7):607–16.
[89] Baran G, Sari A. Phase change and heat transfer characteristics of a eutectic mixture of palmitic and stearic acids as PCM in a latent heat storage system. Energy Conversion and Management 2003;44:3227–46.
[90] Fukai J, Hamada Y, Morozumi Y, Miyatake O. Improvement of thermal characteristics of latent heat thermal energy storage units using carbon-fibre brushes: experiments and modeling. Heat and Mass Transfer 2003;46:4513–25.
[91] Silva PD, Goncalves LC, Pires L. Transient behaviour of a latent-heat thermal energy store: numerical and experimental studies. Applied Energy 2002;73: 83–98.
[92] Sarı A. Thermal characteristics of a eutectic mixture of myristic and palmitic acids as phase change material for heating applications. Applied Thermal Engineering 2003;23:1005–17.
[93] Velraj R, Seeniraj RV, Hafner B, Faber C, Swharzer K. Heat transfer enhancement in a latent heat storage system. Solar Energy 1999;65(3):171–80.
[94] Ismail KAR, Alves CLF, Modesto MS. Numerical and experimental study on the solidification of PCM around a vertical axially finned isothermal cylinder. Applied Thermal Engineering 2001;21:53–77.
[95] Hasan A. Phase change material energy storage system employing palmitic acid. Solar Energy 1994;52(2):143–54.
[96] Agyenim F. PhD Thesis: The development of medium temperature thermal energy storage for cooling applications, University of Ulster; 2007.
[97] Choi JC, Kim SD. Heat transfer characteristics of a latent heat storage system using $MgCl_2{\cdot}6H_2O$. Energy 1992;17(12):1153–64.
[98] Agyenim F, Hewitt N, Eames P, Smyth M. Numerical and experimental development of medium temperature thermal energy storage (Erythritol) system for the hot side of $LiBr/H_2O$ air conditioning applications. In: World Renewable Energy Congress 2008; 2008.
[99] Agyenim F, Eames P, Smyth M. Heat transfer enhancement in medium temperature thermal energy storage system using a multitube heat transfer array. Renewable Energy 2010;35(1):198–207.
[100] Agyenim F, Eames P, Smyth M. A comparison of heat transfer enhancement in a medium temperature thermal energy storage heat exchanger using fins. Solar Energy 2009;83(9):1509–20.
[101] Gong Z, Mujumdar AS. Finite-element analysis of cyclic heat transfer in a shell and tube latent heat energy storage exchanger. Applied Thermal Engineering 1997;17(4):583–91.
[102] Horbaniuc B, Dumitrascua G, Popescub A. Mathematical models for the study of solidification within a longitudinally finned heat pipe latent heat thermal storage system. Energy Conversion & Management 1999;40:1765–74.
[103] Papanicolaou E, Belessiontis V. Transient natural convection in a cylindrical enclosure at high Rayleigh numbers. Heat and Mass Transfer 2001;45:1425–44.

[104] Lecomte D, Mayer D. Design method for sizing a latent heat store/heat exchanger in a thermal system. Applied Energy 1985;21:55–78.
[105] Ismail KAR, Abugderah MM. Performance of a thermal storage system of the vertical tube type. Energy Conversion & Management 2000;41:1165–90.
[106] Ismail KAR, Silva MGE. Numerical solution of the phase change problem around a horizontal cylinder in the presence of natural convection in the melt region. Heat and Mass Transfer 2003;46:1791–9.
[107] Bansal NK, Buddhi D. An analytical study of a latent heat storage system in a cylinder. Energy Conversion Management 1992;33(4):235–42.
[108] Zhang Z, Bejan A. The problem of time-dependent natural convection melting with conduction in the solid. Heat Mass Transfer 1989;32(12):2447–57.
[109] Sparrow EM, Larson ED, Ramsey JW. Freezing on a finned tube for either conduction-controlled or natural convection-controlled heat transfer. International Journal of Heat and Mass Transfer 1981;24:273–84.
[110] Sasaguchi K, Takeo H. Effect of the orientation of a finned surface on the melting of frozen porous media. Heat and Mass Transfer 1994;37(1):13–26.
[111] Zhang Y, Faghri A. Heat transfer enhancement in latent heat thermal energy storage system by using the internally finned tube. International Journal of Heat Mass Transfer 1996;39(15):3165–73.
[112] Velraj R, Seeniraj RV, Hafner B, Faber C, Schwarzer K. Experimental analysis and numerical modelling of inward solidification on a finned vertical tube for a latent heat storage unit. Solar Energy 1997;60(5):281–90.
[113] Trelles JP, Dufly JJ. Numerical simulation of porous latent heat thermal energy storage for thermoelectric cooling. Applied Thermal Engineering 2003;23: 1647–64.
[114] Hoogendoorn CJ, Bart GCJ. Performance and modelling of latent heat stores. Solar Energy 1992;48(1):53–8.
[115] Mettawee ES, Assassa GMR. Thermal conductivity enhancement in a latent heat storage system. Solar Energy 2007;81:839–45.
[116] Griffiths PW, Eames PC. Performance of chilled ceiling panels using phase change material slurries as the heat transport medium. Applied Thermal Engineering 2007;27:1756–60.
[117] Hawlader MNA, Uddin MS, Khin MM. Microencapsulated PCM thermal-energy storage system. Applied Energy 2003;74:195–202.
[118] Hendra R, Hamdani, Mahlia TMI, Masjuki HH. Thermal and melting heat transfer characteristics in a latent heat storage system using mikro. Applied Thermal Engineering 2005;25:1503–15.
[119] Chow LC, Zhong JK, Beam JE. Thermal conductivity enhancement for phase change storage media. International Communications in Heat and Mass Transfer 1996;23(1):91–100.
[120] Lamberg P, Siren K. Approximate analytical model for solidification in a finite PCM storage with internal fins. Applied Mathematical Modelling 2003;27:491–513.
[121] Inaba H, Dai C, Horibe A. Natural convection heat transfer of microemulsion phase-change-material slurry in rectangular cavities heated from below and cooled from above. International Journal of Heat and Mass Transfer 2003;46(23):4427–38.
[122] Liu Z, Sun X, Ma C. Experimental investigations on the characteristics of melting processes of stearic acid in an annulus and its thermal conductivity enhancement by fins. Energy Conversion and Management 2005;46:959–69.
[123] Lamberg P. Approximate analytical model for two-phase solidification problem in a finned phase-change material storage. Applied Energy 2004;77:131–52.
[124] Matsuda H, Ona E, Kojima Y, Ozawa S, Yabe M, Kakiuchi H, et al. Enhancement of phase change of a high temperature PCM with the aid of ultrasonic energy, IEA, ECES IA Annex 17, Advanced thermal energy storage through phase change materials and chemical reactions—feasibility studies and demonstration projects. 3rd Workshop, 1–2 October 2002, Tokyo, Japan.
[125] Hu X, Zhang Y. Novel insight and numerical analysis of convective heat transfer enhancement with microencapsulated phase change material slurries: laminar flow in a circular tube with constant heat flux. International Journal of Heat and Mass Transfer 2002;45(15):3163–72.
[126] Fukai J, Hamada Y, Morozumi Y, Miyatake O. Effect of carbon-fibre brushes on conductive heat transfer in phase change materials. Heat and Mass Transfer 2002;45:4781–92.
[127] Henze RH, Humphrey JAC. Enhanced heat conduction in phase-change thermal energy storage devices. Heat Mass Transfer 1981;24:459–74.
[128] El-Dessouky H, Al-Juwayhel F. The effectiveness of a thermal energy storage system using phase change materials. Energy Conversion Management 1997;38(6):601–17.
[129] Petukhov BS. Heat transfer and friction in turbulent pipe flow with variable physical properties. Advances in Heat Transfer 1970;6:503–64.
[130] Gnielinski V. New equations for heat and mass transfer in turbulent pipes and channels flow. International Chemical Engineering 1976;16:359–68.
[131] Edwards DP, Jensen MK. Pressure drop and heat transfer predictions of turbulent flow in longitudinally finned tubes. Advances in Enhanced Heat Transfer 1994;287:17–23.
[132] Saxena S, Subrahmaniyam S, Sarkah MK. A preliminary model for phase change thermal energy storage in a shell and tube heat exchanger. Solar Energy 1982;29(3):257–63.
[133] Rohsenow WM, Harnett JP, Ganic EN. Handbook of Heat Transfer Fundamentals, 2nd ed., New York: McGraw-Hill; 1985.
[134] Li H, Hsieh CK, Goswami DY. Conjugate heat transfer analysis of fluid flow in a phase-change energy storage unit. Numerical Methods for Heat & Fluid Flow 1996;6(3):77–90.
[135] Morgan K. A numerical analysis of freezing and melting with convection. Computer Methods in Applied Mechanics and Engineering 1981;28(3):275–84.